Attitude Control of Unmanned Aerial Vehicle Based on Sliding Mode Technique with Parameter Estimation

A. A. Akbari*
Department of Mechanical Engineering,
University of Ferdowsi University of Mashhad, Iran,
E-mail: Akbari@um.ac.ir, a.a.akbari@gmail.com
*Corresponding author

S. Amini
Department of Mechanical Engineering,
University of Ferdowsi University of Mashhad, Iran,
E-mail: amini.samane@ymail.com

Received: 9 December 2016, Revised: 29 January 2017, Accepted: 14 February 2017

Abstract: An adaptive robust controller for nonlinear and coupling dynamic of aerial vehicle has been presented. In this paper an adaptive sliding mode controller (ASMC) is integrated to design the attitude control for the inner loops of nonlinear coupling dynamic of Unmanned Aerial Vehicle (UAV) in the presence of parametric uncertainties and disturbances. In the proposed scheme, the adaptation laws can estimate the unknown uncertain parameters and external disturbances, while the sliding mode control is used to ensure the fast response and robustify the control design against unmodeled dynamics with a small control effort. The synthesis of the adaptation laws is based on the positivity and Lyapunov design principle. In comparison with other sliding mode approaches, the approach does not need the upper bound of parametric uncertainty and disturbances. The navigation outer loops of small UAV instead is based on PIDs to control altitude and heading. Simulation results demonstrate that the proposed controller can stabilize the nonlinear system and also it has stronger robustness with respect to the model uncertainties and gust disturbance.

Keywords: Adaptation laws, Aerial vehicle, Nonlinear dynamic, Sliding mode control

Reference: Akbari. A. A., Amini, S., "Attitude Control of Unmanned Aerial Vehicle Based on Sliding Mode Technique with Parameter Estimation", Int J of Advanced Design and Manufacturing Technology, Vol. 10/ No. 2, 2017, pp. 49–60.

Biographical notes: A. A. Akbari received his PhD in Mechanical Engineering from Chiba University in 2003. He is currently Assistant Professor at the Department of Mechanical Engineering, Ferdowsi University of Mashhad, Iran. His current research interest includes robotic and control, intelligent manufacturing. **S. Amini** is a graduate MSc student of Mechanical engineering at the Ferdowsi University of Mashhad, Iran. Her current research focuses on simulation of dynamic systems, robotic and control and optimization.

1 INTRODUCTION

An unmanned aerial vehicle (UAV) is a powered, aerial vehicle that does not carry a human operator, uses aerodynamic forces to provide vehicle lift, can fly autonomously or piloted remotely, and can carry payloads [1]. In recent years, micro and small UAVs have attracted many researchers and developers around the world since they had the potential to be used in military and civilian applications, e.g. traffic assistance, surveillance, mapping, inspection power lines, oil pipelines and etc. [2-3]. The attitude control system design of UAVs is a challenging task due to various difficulties faced when working with them. These systems are multi-input multi output (MIMO), nonlinear, coupled between the longitudinal and lateral dynamic, and very sensible to external disturbances [4]. Moreover, parametric uncertainties characteristics may also cause more complications during the design of such attitude control systems.
In the last few decades, much research effort has been devoted to the design or improvement of the controller of uncertain systems. The author of [5] proposed an L_1 adaptive controller as autopilot inner loop controller candidate. Navigation outer loop parameters are regulated via PID control method. The paper demonstrates that, if an L_1 algorithm is considered for the inner loop, no retuning or gain scheduling is required, even if a nonlinear complete system is considered. A robust adaptive terminal sliding mode control law with adaptive algorithms in [6] is presented to solve the six-degree-of-freedom tracking control problem of the leader-follower spacecraft formation. The proposed control law is proved to be able to drive the relative translational and rotational motion to the desired trajectory in finite time despite the presence of model uncertainties and external disturbances.
The results show that using the presented controllers, the desired tracking performance in the investigated problem can be achieved. In [7] an adaptive backstepping design for a class unmanned helicopters with parametric uncertainties. The control objective is to let the helicopter track some pre-defined position and yaw trajectories. The proposed controller combines the backstepping method with online parameter update laws to achieve the control objective. Numerical simulations demonstrate that the controller can achieve good tracking performance in the presence of the parametric uncertainties. In [8], the fuzzy sliding mode control is proposed to design the altitude hold mode autopilot for a UAV which is non-minimum phase, and its model includes both parametric uncertainties and unmodeled nonlinear dynamics. In [9] the authors presented an adaptive neural network controller using backstepping technique for autonomous flight. The main feature of [9] is that the adaptive controller is designed assuming that all of the nonlinear functions of the system have uncertainties and the neural network weights are adjusted adaptively via Lyapunov theory.
Sliding mode control has been suggested as a powerful approach for control systems with nonlinearities, uncertain dynamics and bounded input disturbances [10]. The most distinguished feature of SMC is its ability to provide fast error convergence and strong robustness for control systems in the sense that the closed loop systems are completely insensitive to nonlinearities and uncertain dynamics [11]. However, the bounds of system uncertainties are required for sliding mode control and this drawback attenuates the control system performance [12]. The combined adaptive sliding mode controllers (robust adaptive controllers) have been studied in [7-13-14-15] as a method to overcome the drawbacks of adaptive control and SMC. The idea is to use the adaptive control to estimate the unknown parameters of the dynamical system and to use the SMC to overcome the un-modelled dynamics and external disturbances. Adaptive sliding mode control (ASMC), the combination of adaptive control method and SMC approach, is more flexible and convenient in controller design than SMC. In [16] an adaptive robust nonlinear controller is developed and applied to a quadrotor to attenuate the chattering effects and to achieve finite time convergence and robustness aims. In [17] adaptive sliding mode control has been used for trajectory following underground effects.
In this paper, a sliding mode control approach based on adaptive control is investigated for nonlinear coupling dynamic of the inner loop fixed wing UAV in the presence of different parametric uncertainties and disturbances caused by the environment. The contribution of the present paper is the validation of the controller parameters when a nonlinear complete aircraft model is considered (both longitudinal and latero planes), including model uncertainties and unmodeled dynamics. In the proposed scheme, sliding mode control law parameters due to uncertainty are assumed to be unknown and are estimated via adaptation laws. The global asymptotical stability of the closed-loop system is proved by a Lyapunov based stability analysis. Furthermore, navigation outer loop parameters are regulated via PID controllers.
In comparison with other control approaches, the proposed method benefits from high robustness in presence of different parametric uncertainties, i.e. aerodynamic coefficients, inertia moment and configuration parameters uncertainties and disturbances caused by the environment such as wind. Furthermore, the chattering phenomenon in sliding mode control is avoided by using saturation function [18]. The paper is organized as follows: In section 2, dynamic and

kinematic equations of small fixed wing UAV for dynamic modelling are introduced. In section 3, the control strategy for nonlinear dynamics of UAV and the adaptive sliding mode controller theory is presented. Simulation results are analyzed in section 4. Finally, conclusions are presented in section 5.

2 MODELING FOR UAV'S MOTION

The air vehicle is modelled as a standard system with the main assumptions that UAV is a rigid body with a symmetric geometry and center of UAV mass position is fixed [19]. The Earth-fixed $(X_E Y_E Z_E)$ and the body-fixed $(X_B Y_B Z_B)$ are two reference coordinate frames most frequently used to describe the motion of an air vehicle, as shown in Fig. 1. The Body-fixed frame is attached to the vehicle. Its origin is normally at the centre of gravity. The motion of the Body-fixed frame is described relative to the Earth-fixed frame. In order to describe the motion of an UAV in 6 DOF, six independent coordinates representing position and attitude are necessary. The kinematics can be described by its position, orientation, linear and angular velocity over time. The position vector is given by $[x, y, z]$ in Earth frame, with x pointing to true north, y pointing east and z pointing downwards. Velocities are described in body axes with linear velocity $[u, v, w]$, where u is the longitudinal velocity, v is the lateral velocity and w is the vertical velocity. The major attitude tracking variables are described by Euler angles $[\phi, \theta, \psi]$, with roll angle, pitch angle and yaw angle respectively. The angular velocity is given by $[p, q, r]$, where p, q and r is the roll, pitch and yaw angular velocity, respectively.

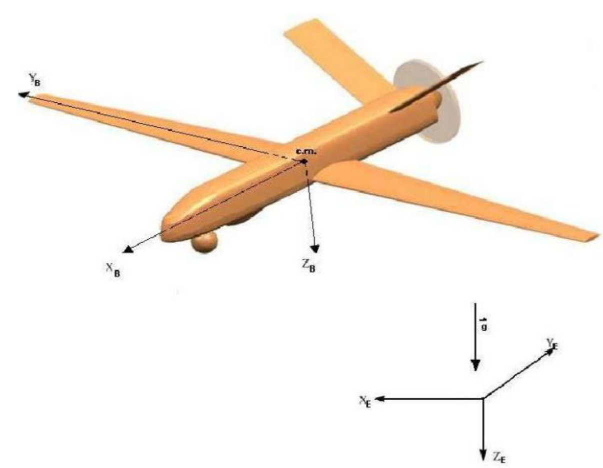

Fig. 1 The Earth-fixed and the Body-fixed coordinate systems [20]

Air vehicle equations of motion are derived from Newton-Euler formulation. They basically describe the air vehicle as a rigid body moving through the space. The detailed of these equations is given in many text books and other studies such as [21-22]. The mathematical model of an UAV's translational and rotational motion can be expressed as follows,
Translational equations of motion:

$$\begin{aligned}
\dot{u} &= rv - qw + \tfrac{1}{m}\left(X - mg\sin\theta + T\right)\\
\dot{v} &= pw - ru + \tfrac{1}{m}\left(Y + mg\cos\theta\sin\phi\right)\\
\dot{w} &= qu - pv + \tfrac{1}{m}\left(Z + mg\cos\theta\cos\phi\right)
\end{aligned} \tag{1}$$

Rotational equations of motion:

$$\begin{aligned}
\dot{p} &= \Gamma_1 pq - \Gamma_2 qr + \Gamma_3 L + \Gamma_4 N\\
\dot{q} &= \Gamma_5 pr - \Gamma_6 (p^2 - r^2) + \tfrac{1}{I_y} M\\
\dot{r} &= \Gamma_7 pq - \Gamma_1 qr + \Gamma_4 L + \Gamma_8 N
\end{aligned} \tag{2}$$

Where T is the UAV thrust force, g is the gravitational acceleration, m is the UAV mass, (X, Y, Z) are the aerodynamic forces and (L, M, N) are the aerodynamic moments. Additionally, Γ_i can be expressed as,

$$\begin{aligned}
&\Gamma = I_{xx} I_{zz} - I_{xz}^2, \Gamma_1 = \frac{I_{xz}\left(I_{xx} - I_{yy} + I_{zz}\right)}{\Gamma},\\
&\Gamma_2 = \frac{I_{zz}\left(I_{zz} - I_{yy}\right) + I_{xz}^2}{\Gamma}, \Gamma_3 = \frac{I_{zz}}{\Gamma}, \Gamma_4 = \frac{I_{xz}}{\Gamma},\\
&\Gamma_5 = \frac{I_{zz} - I_{xx}}{\Gamma}, \Gamma_6 = \frac{I_{xz}}{I_{yy}}
\end{aligned} \tag{3}$$

Where I_{ij} represents the inertia moments. The aerodynamic forces and moments are functions of all the considered states. Aerodynamic forces and moments can be calculated by means of aerodynamic coefficients as,

$$\begin{aligned}
\begin{pmatrix} X \\ Y \\ Z \end{pmatrix} &= \frac{1}{2}\rho V^2 S \begin{pmatrix} C_X \\ C_Y \\ C_Z \end{pmatrix}\\
\begin{pmatrix} L \\ M \\ N \end{pmatrix} &= \frac{1}{2}\rho V^2 S \begin{pmatrix} bc_l \\ \bar{c}c_m \\ bc_n \end{pmatrix}
\end{aligned} \tag{4}$$

Where $V = \sqrt{u^2 + v^2 + w^2}$ is the airspeed and wing surface area S, the wingspan b, the mean aerodynamic cord $\bar{c}$ and the air density ρ, are considered constant parameters. In general, the aerodynamic coefficients are under look-up table from wind tunnel data measurements [23]. The dimensionless coefficients in the force/moment expressions can be decomposed in the following set of equations [24],

$$
\begin{aligned}
C_X &= C_L \sin\alpha - C_D \cos\alpha, \\
C_Y &= C_{Y_\beta} + C_{Y_{\delta_r}} \delta_r + \frac{b}{2V}\left(C_{Y_p} p + C_{Y_r} r\right), \\
C_Z &= -C_D \sin\alpha - C_L \cos\alpha, \\
c_l &= c_{l_\beta}\beta + c_{l_{\delta_a}}\delta_a + c_{l_{\delta_r}}\delta_r + \frac{b}{2V}\left(c_{l_p} p + c_{l_r} r\right), \\
c_m &= c_{m0} + c_{m_\alpha}\alpha + c_{m_{\delta_e}}\delta_e + \frac{\bar{c}}{2V}\left(c_{m_q} q + c_{m_{\dot\alpha}}\dot\alpha\right), \\
c_n &= c_{n_\beta}\beta + c_{n_{\delta_a}}\delta_a + c_{n_{\delta_r}}\delta_r + \frac{b}{2V}\left(c_{n_p} p + c_{n_r} r\right)
\end{aligned} \tag{5}
$$

Where the lift (C_L) and the drag (C_D) coefficients are calculated using the following equations,

$$
\begin{aligned}
C_L &= C_{L0} + C_{L_\alpha}\alpha + C_{L_{\delta_e}}\delta_e + \frac{\bar{c}}{2V} C_{L_q}, \\
C_D &= C_{D0} + C_{D_{\delta_r}}\delta_r + C_{D_{\delta_e}}\delta_e + \frac{C_L - C_{L_{\min}}}{\pi e AR}
\end{aligned}
$$

Where α, β are the attack and the sideslip angles, e is the Oswalds efficient number and AR is the aspect ratio calculated as $AR = b^2/2$ [24]. The conventional aerodynamic control surface deflection variable are defined by aileron (δ_a), elevator (δ_e) and rudder (δ_r) which respectively are caused by rolling moment, pitching moment and yawing moment. It is also prudent to include a throttle variable, denoted by (δ_T), that is related to the output magnitude of the UAV thrust. Euler angles are one of the standard specifications used for expressing the orientation of the body-fixed frame relative to the Earth-fixed frame. Kinematical relationship between Euler angles and body-fixed angular rates are given as,

$$
\begin{aligned}
\dot\phi &= p + \tan\theta(q\sin\phi + r\cos\phi) \\
\dot\theta &= q\cos\phi - r\sin\phi \\
\dot\psi &= \sec\theta(q\sin\phi + r\cos\phi)
\end{aligned} \tag{6}
$$

Another set of equations, navigation equations which relate translational velocity components in body-fixed axes to Earth-fixed axes components are given as,

$$
\begin{aligned}
\dot x_E &= u\cos\psi\cos\theta + v(\cos\psi\sin\theta\sin\phi - \sin\psi\cos\phi) \\
&\quad + w(\cos\psi\sin\theta\cos\phi + \sin\psi\sin\phi) \\
\dot y_E &= u\sin\psi\cos\theta + v(\sin\psi\sin\theta\sin\phi + \cos\psi\cos\phi) \\
&\quad + w(\sin\psi\sin\theta\cos\phi - \cos\psi\sin\phi) \\
\dot h &= u\sin\theta - v\sin\phi\cos\theta - w\cos\phi\cos\theta
\end{aligned} \tag{7}
$$

3 CONTROL SYSTEM DESIGN

In this section, the control objective is to design a control strategy that permits the small UAV to track its desired trajectory. As illustrated in Fig. 2, the multivariable dynamic control system for a fixed wing UAV is divided into longitudinal and lateral plans. The longitudinal plane controls the pitch angle θ in the inner loop and the altitude h in the outer loop by elevator control surface δ_e and controls the speed by throttle δ_t. The lateral planes controls the roll angle ϕ in the inner loop and heads angle ψ in the outer loop by aileron control surface δ_a [25]. In classical SMC approach, the control effort is designed on the basis of the upper bounds of system uncertainties, which can guarantee the reachability of sliding mode, but a conservative high gain control effort is used in the whole control process while uncertainties may rarely run on the bonds in practical [26].

In this paper, the uncertain parameters are estimated with properly designed adaptive law and the robust control items related to SMC is used to ensure the fast response and robustify the control design against unmodeled dynamics with a small control effort. The control problem is to design the control input, making the attitude motion track the command attitude angles effectively and precisely in the presence of parameter uncertainty and external disturbance. In this paper, the adaptive sliding mode controller is chosen to control the inner navigation loops, those need a faster response and are more prone to be affected by model uncertainties due to platform geometric and external disturbances. Altitude and heading outer navigation loops are instead controlled by simple PIDs. It should be noted that although no rudder is used, the response on the heading angles is still satisfying with aileron control.

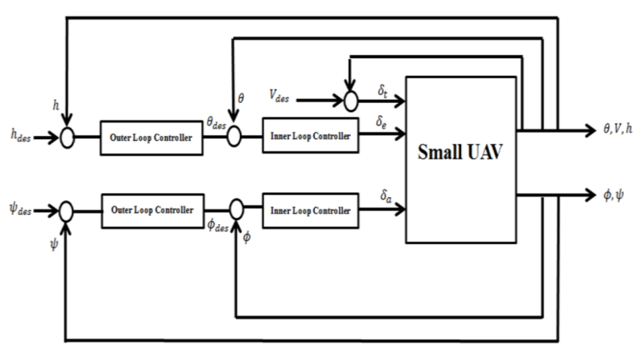

Fig. 2 The control scheme of Small UAV

3.1. Sliding Mode Controller Design

In general, sliding mode controller design is divided into two steps. The first step is to define the sliding surface. The second step is to determine a reaching law such that the system will get to and maintain on the intersection of the sliding surface [26]. The suitable sliding surface for inner loops of longitudinal and lateral planes can be described as,

$$S_{long}(t) = e_\theta + c_1 q \quad (8)$$

$$S_{lat}(t) = e_\phi + c_2 p \quad (9)$$

Where c_1, c_2 are positive design parameters, $e_\theta = \theta(t) - \theta_d(t)$ and $e_\phi = \phi(t) - \phi_d(t)$ are the pitch and roll angle tracking error respectively and also θ_d and ϕ_d are the desired pitch and roll angle respectively. The sliding surfaces can then be differentiated with respect to time as :

$$\dot{S}_{long}(t) = \dot{e}_\theta + c_1 \dot{q} \quad (10)$$

$$\dot{S}_{lat}(t) = \dot{e}_\phi + c_2 \dot{p} \quad (11)$$

Substituting (5) into (4) and then (4) into (2) and also substituting $\dot{q}$ and $\dot{p}$ from (2) into (10) and (11) respectively yields :

$$\dot{S}_{long}(t) = \dot{e}_\theta + c_1\Big(\Gamma_5 pr - \Gamma_6\left(p^2 - r^2\right) + \frac{\rho V^2 Sc}{2I_y}\Big(C_{m0} + C_{m\alpha}\alpha + C_{mq}\frac{cq}{2V} + C_{m\delta_e}\delta_e\Big)\Big) \quad (12)$$

$$\dot{S}_{lat}(t) = \dot{e}_\phi + c_2\Big(\Gamma_1 pq - \Gamma_2 qr + \frac{\rho V^2 Sb}{2}\Big(C_{p_\beta}\beta + C_{p_p}\frac{bp}{2V} + C_{p_r}\frac{br}{2V} + C_{p_{\delta_a}}\delta_a\Big)\Big) \quad (13)$$

Where,

$$C_{p_\beta} = \Gamma_3 C_{l_\beta} + \Gamma_4 C_{n_\beta},\ C_{p_p} = \Gamma_3 C_{l_p} + \Gamma_4 C_{n_p},$$
$$C_{p_r} = \Gamma_3 C_{l_r} + \Gamma_4 C_{n_r},\ C_{p_{\delta_a}} = \Gamma_3 C_{l_{\delta_a}} + \Gamma_4 C_{n_{\delta_a}}$$

Another form for the expression of $\dot{S}_{long}$ and $\dot{S}_{lat}(t)$ is:

$$\dot{S}_{long}(t) = \dot{e}_\theta + \frac{c_1 V^2}{\sigma_1}\Big(\sigma_2\frac{pr}{V^2} - \sigma_3\frac{p^2 - r^2}{V^2} - \sigma_4 - \sigma_5\alpha - \sigma_6\frac{q}{V} - \delta_e\Big) \quad (14)$$

$$\dot{S}_{lat}(t) = \dot{e}_\phi + \frac{c_2 V^2}{\tau_1}\Big(\tau_2\frac{pq}{V^2} - \tau_3\frac{qr}{V^2} - \tau_4\beta - \tau_5\frac{p}{V} + \tau_6\frac{r}{V} - \delta_a\Big) \quad (15)$$

Where vectors $\sigma_i, \tau_i\ (i = 1,2,3,4,5,6)$ are given as follows :

$$\sigma = \left[\frac{-2I_y}{\rho ScC_{m\delta_e}} \quad \frac{-2I_y\Gamma_5}{\rho ScC_{m\delta_e}} \quad \frac{-2I_y\Gamma_6}{\rho ScC_{m\delta_e}} \quad \frac{C_{m0}}{C_{m\delta_e}} \quad \frac{C_{m\alpha}}{C_{m\delta_e}} \quad \frac{cC_{mq}}{2C_{m\delta_e}}\right] \quad (16)$$

$$\tau = \left[\frac{-2}{\rho SbC_{p_{\delta_a}}} \quad \frac{-2\Gamma_1}{\rho SbC_{p_{\delta_a}}} \quad \frac{-2\Gamma_2}{\rho SbC_{p_{\delta_a}}} \quad \frac{-C_{p_\beta}}{C_{p_{\delta_a}}} \quad \frac{-bC_{p_p}}{2C_{p_{\delta_a}}} \quad \frac{bC_{p_r}}{2C_{p_{\delta_a}}}\right] \quad (17)$$

The output signal of the sliding mode controller is composed of two terms as, $u = u_{eq} + u_{sw}$,Where u_{eq} is the signal of the equivalent part and u_{sw} is the signal of the switching part. The switching part of sliding mode control takes the form $k\,\mathrm{sgn}(s)$, in which $\mathrm{sgn}(s)$ is a sign function and k is a positive constant. Now, consider a sliding mode controller described as :

$$u_{long} = \sigma\Delta^T + k_1\,\mathrm{sgn}(S_{long}) \quad (18)$$

$$u_{lat} = \tau\nabla^T + k_2\,\mathrm{sgn}(S_{lat}) \quad (19)$$

Where,

$$\Delta = \left[\frac{\dot{e}_\theta}{c_1 V^2} \quad \frac{pr}{V^2} \quad -\frac{\left(p^2 - r^2\right)}{V^2} \quad -1 \quad -\alpha \quad -\frac{q}{V}\right] \quad (20)$$

$$\nabla = \left[\frac{\dot{e}_\phi}{c_2 V^2} \quad \frac{pq}{V^2} \quad -\frac{qr}{V^2} \quad -\beta \quad -\frac{p}{V} \quad -\frac{r}{V}\right] \quad (21)$$

The stability of the sliding mode control laws will be reviewed in the following.

Theorem 1. Consider the rotational dynamic of a small UAV in equations (2) with sliding surfaces given by equation (8) and (9) .If the control laws of (18) and (19) are implemented, the closed-loop system will be globally and asymptotically stable and the tracking error of attitude UAV converge to zero, i.e. $\lim_{t\to\infty} e_\theta = \lim_{t\to\infty} e_\phi = 0$.

Proof 1. A candidate Lyapunov positive definite function V is defined as :

$$V = \frac{1}{2}S_{long}(t)^2 + \frac{1}{2}S_{lat}(t)^2 \tag{22}$$

Then, if $\dot V \le 0$, asymptotic Lyapunov stability will be guaranteed. In view of (13) and (14), calculating the derivative of V yields ;

$$\begin{aligned}\dot V &= S_{long}(t)\dot S_{long}(t) + S_{lat}(t)\dot S_{lat}(t)\\ &= S_{long}(t)\Bigg(\dot e_\theta + \frac{c_1 V^2}{\sigma_1}\Bigg(\sigma_2\frac{pr}{V^2} - \sigma_3\frac{p^2-r^2}{V^2} - \sigma_4\\ &-\sigma_5\alpha - \sigma_6\frac{q}{V} - \delta_e\Bigg)\Bigg) + S_{lat}(t)\Bigg(\dot e_\phi + \frac{V^2 c_2}{\tau_1}\Bigg(\tau_2\frac{pq}{V^2}\\ &-\tau_3\frac{qr}{V^2} - \tau_4\beta - \tau_5\frac{p}{V} + \tau_6\frac{r}{V} - \delta_a\Bigg)\Bigg)\end{aligned} \tag{20}$$

By substituting the control laws (17) and (18) into δ_e and δ_a respectively and simplifying the equations (20), we obtain :

$$\dot V \le -k_1\left|S_{long}(t)\right| - k_2\left|S_{lat}(t)\right| \tag{21}$$

Obviously, $\dot V \le 0$. Hence, based on the Lyapunov stability theory, the theorem is proved.

3.2. SMC with Adaptive Method

It is assumed that the components of vectors σ and τ due to different parametric uncertainties, i.e. aerodynamic coefficients, inertia moment and configuration parameters uncertainties are unknown. Therefore, the sliding mode control laws that were designed in the previous section are improved by means of adaptive laws. Consider adaptive sliding mode control laws as :

$$u_{long} = \hat\sigma\Delta^T + k_1\,\mathrm{sgn}(s_{long}) \tag{22}$$

$$u_{lat} = \hat\tau\nabla^T + k_2\,\mathrm{sgn}(s_{lat}) \tag{23}$$

Let $\hat\sigma$ and $\hat\tau$ be the estimation for σ and τ respectively which are updated using the following adaptation laws :

$$\dot{\tilde\sigma}_i = \eta S_{long}(t)\frac{c_1 V^2}{\sigma_1}\Delta_i \quad i = 1:6 \tag{24}$$

$$\dot{\tilde\tau}_i = \mu S_{lat}(t)\frac{c_2 V^2}{\tau_1}\nabla_i \quad i = 1:6 \tag{25}$$

Where η and μ are positive design parameters, Δ_i and ∇_i are the ith elements of the vectors Δ, ∇ and also $\tilde\sigma$ and $\tilde\tau$ are defined as :

$$\tilde\sigma = \hat\sigma - \sigma,\quad \tilde\tau = \hat\tau - \tau \tag{26}$$

Note that $\tilde\sigma$ and $\tilde\tau$ are the estimated value of σ and τ respectively, and also $\dot{\tilde\sigma}$ and $\dot{\tilde\tau}$ can be represented as $\dot{\hat\sigma}$ and $\dot{\hat\tau}$ with an assumption that σ and τ changes slowly. According to the above analysis, the following theorem can be proposed.

Theorem 2. Consider rotational dynamic of a small UAV described by equation (2) with unknown parameters. If control laws are designed as equations (22) and (23) with the adaptation laws (24) and (25), the trajectory of the system will track the desired trajectory and the system is globally asymptotically stable in finite time under the presence of uncertainties and disturbances.

Proof 2. To prove the robustness and stability of the proposed controller and to derive the estimation laws for the unknown parameters, the following Lyapunov functions are considered :

$$V_1 = \frac{1}{2}S_{long}(t)^2 + \frac{1}{2\eta}\sum_{i=1}^{6}\tilde\sigma_i^2 \tag{27}$$

$$V_2 = \frac{1}{2}S_{lat}(t)^2 + \frac{1}{2\mu}\sum_{i=1}^{6}\tilde\tau_i^2 \tag{28}$$

At first consider stability for ASMC method of longitudinal plane. Therefore calculating the derivative of V_1 along the system (13) yields :

$$\begin{aligned}\dot V_1 &= S_{long}(t)\dot S_{long}(t) + \frac{1}{\eta}\sum_{i=1}^{6}\tilde\sigma_i\dot{\tilde\sigma}_i\\ &= S_{long}(t)\Bigg(\dot e_\theta + \frac{c_1V^2}{\sigma_1}(\sigma_2\frac{pr}{V^2} - \sigma_3\frac{p^2-r^2}{V^2}\\ &-\sigma_4 - \sigma_5\alpha - \sigma_6\frac{q}{V} - \delta_e)\Bigg) + \frac{1}{\eta}\sum_{i=1}^{6}\tilde\sigma_i\dot{\tilde\sigma}_i\end{aligned} \tag{29}$$

Substituting (22) into the expression δ_e in (29), we obtain :

$$\begin{aligned}\dot{V}_1 = {} & S_{long}(t)\frac{c_1V^2}{\sigma_1}\left(\sigma_1\left(\frac{\dot{e}_\theta}{c_1V^2}\right)+\sigma_2\frac{pr}{V^2}\right.\\ & -\sigma_3\frac{p^2-r^2}{V^2}-\sigma_4-\sigma_5\alpha-\sigma_6\frac{q}{V}-\hat{\sigma}_1\left(\frac{\dot{e}_\theta}{c_1V^2}\right)\\ & -\hat{\sigma}_2\frac{pr}{V^2}+\hat{\sigma}_3\frac{p^2-r^2}{V^2}+\hat{\sigma}_4+\hat{\sigma}_5\alpha+\hat{\sigma}_6\frac{q}{V}\\ & \left.-k_1 sgn(S_{long})\right)+\frac{1}{\eta}\sum_{i=1}^{6}\tilde{\sigma}_i\dot{\tilde{\sigma}}_i\end{aligned} \tag{30}$$

Regarding expression (26) as the estimated value of σ, we can rewrite the Eq. (30) as follows :

$$\begin{aligned}\dot{V}_1 = {} & S_{long}(t)\frac{c_1V^2}{\sigma_1}\left(-\tilde{\sigma}_1\left(\frac{\dot{e}_\theta}{c_1V^2}\right)-\tilde{\sigma}_2\frac{pr}{V^2}+\right.\\ & \tilde{\sigma}_3\frac{p^2-r^2}{V^2}+\tilde{\sigma}_4+\tilde{\sigma}_5\alpha+\tilde{\sigma}_6\frac{q}{V}\\ & \left.-k_1 sgn(S_{long})\right)+\frac{1}{\eta}\sum_{i=1}^{6}\tilde{\sigma}_i\dot{\tilde{\sigma}}_i\end{aligned} \tag{31}$$

By substituting the adaptation laws (24) into the above equation, we have :

$$\begin{aligned}\dot{V}_1 = {} & S_{long}(t)\frac{c_1V^2}{\sigma_1}\left(-\tilde{\sigma}_1\left(\frac{\dot{e}_\theta}{c_1V^2}\right)-\tilde{\sigma}_2\frac{pr}{V^2}+\right.\\ & \left.\tilde{\sigma}_3\frac{p^2-r^2}{V^2}+\tilde{\sigma}_4+\tilde{\sigma}_5\alpha+\tilde{\sigma}_6\frac{q}{V}-k_1 sgn(S_{long})\right)+\\ & \frac{1}{\eta}\left(\eta S_{long}\frac{c_1V^2}{\sigma_1}\left(\tilde{\sigma}_1\Delta_1+\tilde{\sigma}_2\Delta_2+\tilde{\sigma}_3\Delta_3+\tilde{\sigma}_4\Delta_4+\tilde{\sigma}_5\Delta_5+\tilde{\sigma}_6\Delta_6\right)\right)\end{aligned}$$

Substituting Δ_i from (20) into (31), we obtain :

$$\begin{aligned}\dot{V}_1 = {} & S_{long}(t)\frac{c_1V^2}{\sigma_1}\left(-\tilde{\sigma}_1\left(\frac{\dot{e}_\theta}{c_1V^2}\right)-\tilde{\sigma}_2\frac{pr}{V^2}+\right.\\ & \left.\tilde{\sigma}_3\frac{p^2-r^2}{V^2}+\tilde{\sigma}_4+\tilde{\sigma}_5\alpha+\tilde{\sigma}_6\frac{q}{V}-k_1 sgn(S_{long})\right)+\\ & \frac{1}{\eta}\left(\eta S_{long}\frac{c_1V^2}{\sigma_1}\left(\tilde{\sigma}_1\frac{\dot{e}_\theta}{c_1V^2}+\tilde{\sigma}_2\frac{pr}{V^2}-\tilde{\sigma}_3\frac{p^2-r^2}{V^2}-\tilde{\sigma}_4-\tilde{\sigma}_5\alpha-\tilde{\sigma}_6\frac{q}{V}\right)\right)\end{aligned}$$

Finally, by simplifying the above equation yields :

$$\begin{aligned}\dot{V}_1 &= -\frac{c_1V^2}{\sigma_1}k_1S_{long}(t)\operatorname{sgn}(S_{long}(t))\\ \dot{V}_1 &\le -\frac{c_1V^2}{\sigma_1}k_1\left|S_{long}(t)\right|\end{aligned} \tag{32}$$

The term $\frac{c_1V^2}{\sigma_1}$ on the right hand side of this equation is positive. Hence $\dot{V}_1 \le 0$, and on account of the Lyapunov stability theory, the theorem is proved. Similarly, the derivative of V_2 along the system (14) is then calculated as :

$$\begin{aligned}\dot{V}_2 &= S_{lat}(t)\dot{S}_{lat}(t)+\frac{1}{\mu}\sum_{i=1}^{6}\tilde{\tau}_i\dot{\tilde{\tau}}_i\\ &= S_{lat}(t)\left(\dot{e}_\phi+\frac{c_2V^2}{\tau_1}\left(\tau_2\frac{pq}{V^2}-\tau_3\frac{qr}{V^2}-\tau_4\beta\right.\right.\\ & \quad \left.\left.-\tau_5\frac{p}{V}+\tau_6\frac{r}{V}-\delta_a\right)\right)+\frac{1}{\mu}\sum_{i=1}^{6}\tilde{\tau}_i\dot{\tilde{\tau}}_i\end{aligned} \tag{33}$$

By substituting (23) into the expression δ_a in (29), we have :

$$\begin{aligned}\dot{V}_2 = {} & S_{lat}(t)\frac{c_2V^2}{\tau_1}\left(\tau_1\left(\frac{\dot{e}_\phi}{c_2V^2}\right)+\tau_2\frac{pq}{V^2}-\tau_3\frac{qr}{V^2}\right.\\ & -\tau_4\beta-\tau_5\frac{p}{V}+\tau_6\frac{r}{V}-\hat{\tau}_1\left(\frac{\dot{e}_\phi}{c_2V^2}\right)-\hat{\tau}_2\frac{pq}{V^2}\\ & \left.+\hat{\tau}_3\frac{qr}{V^2}+\hat{\tau}_4\beta+\hat{\tau}_5\frac{p}{V}-\hat{\tau}_6\frac{r}{V}-k_2\operatorname{sgn}(S_{lat})\right)\\ & +\frac{1}{\mu}\sum_{i=1}^{6}\tilde{\tau}_i\dot{\tilde{\tau}}_i\end{aligned} \tag{34}$$

Considering expression (26) as the estimated value of τ, we can express the equation (34) as follows :

$$\begin{aligned}\dot{V}_2 = {} & S_{lat}(t)\frac{c_2V^2}{\tau_1}\left(-\tilde{\tau}_1\left(\frac{\dot{e}_\phi}{c_2V^2}\right)-\tilde{\tau}_2\frac{pq}{V^2}+\tilde{\tau}_3\frac{qr}{V^2}+\right.\\ & \left.\tilde{\tau}_4\beta+\tilde{\tau}_5\frac{p}{V}-\tilde{\tau}_6\frac{r}{V}-k_2\operatorname{sgn}(S_{lat})\right)+\frac{1}{\mu}\sum_{i=1}^{6}\tilde{\tau}_i\dot{\tilde{\tau}}_i\end{aligned} \tag{35}$$

With substituting the adaptation laws (25) yields :

$$\begin{aligned}\dot{V}_2 = {} & S_{lat}(t)\frac{c_2V^2}{\tau_1}\left(-\tilde{\tau}_1\left(\frac{\dot{e}_\phi}{c_2V^2}\right)-\tilde{\tau}_2\frac{pq}{V^2}+\tilde{\tau}_3\frac{qr}{V^2}+\right.\\ & \left.\tilde{\tau}_4\beta+\tilde{\tau}_5\frac{p}{V}-\tilde{\tau}_6\frac{r}{V}-k_2\operatorname{sgn}(S_{lat})\right)\\ & +\frac{1}{\mu}\left(\mu S_{lat}(t)\frac{c_2V^2}{\tau_1}\left(\tilde{\tau}_1\nabla_1+\tilde{\tau}_2\nabla_2+\tilde{\tau}_3\nabla_3+\tilde{\tau}_4\nabla_4+\tilde{\tau}_5\nabla_5+\tilde{\tau}_6\nabla_6\right)\right)\end{aligned}$$

Substituting ∇_i from (21) into (35), we obtain :

$$\dot{V}_2 = S_{lat}(t)\frac{c_2V^2}{\tau_1}\left(-\tilde{\tau}_1\left(\frac{\dot{e}_\phi}{c_2V^2}\right)-\tilde{\tau}_2\frac{pq}{V^2}+\tilde{\tau}_3\frac{qr}{V^2}+\right.$$

$$\tilde{\tau}_4\beta + \tilde{\tau}_5\frac{p}{V} - \tilde{\tau}_6\frac{r}{V} - k_2\,\text{sgn}(S_{lat})\Bigg)$$
$$+\frac{1}{\mu}\left(\mu S_{lat}(t)\frac{c_2V^2}{\tau_1}\left(\tilde{\tau}_1\frac{\dot{e}_\phi}{c_2V^2}+\tilde{\tau}_2\frac{pq}{V^2}-\tilde{\tau}_3\frac{qr}{V^2}-\tilde{\tau}_4\beta-\tilde{\tau}_5\frac{p}{V}-\tilde{\tau}_6\frac{r}{V}\right)\right)$$

Finally, by simplifying the above equation, we have :

$$\dot{V}_2 = -\frac{c_2V^2}{\tau_1}k_2 S_{lat}(t)\,\text{sgn}(S_{lat}(t))$$
$$\dot{V}_2 \le -\frac{c_2V^2}{\tau_1}k_2\left|S_{lat}(t)\right| \qquad (36)$$

Similarly, as $\frac{c_2V^2}{\tau_1}$ is positive, $\dot{V}_2 \le 0$. Therefore, based on the Lyapunov stability theory, the theorem is proved.

Remark 1. In order to avoid the chattering phenomenon due to the imperfect implementation of the sign function in the control laws (22) and (23), the following saturation function is replaced [27] :

$$\text{sat}(S) = \begin{cases} 1 & S > \varepsilon \\ S & |S| \le \varepsilon \\ -1 & S < \varepsilon \end{cases} \qquad (37)$$

In which ε is a small constant.

4 SIMULATION RESULT AND DISCUSSION

In this section, we present results of applying the proposed control scheme to a full 6 degree of freedom model of UAV. A mathematical model of a small fixed wing UAV has been derived from [22] and implemented in Matlab Simulink environment.

Table 1 The Small fixed wing UAV parameters [24]

Parameter	Value	Unit
Weight	1.595	*kg*
Span	1.27	*m*
Wing surface	0.3097	m^2
Mean aerodynamic chord	0.25	*m*
Inertia moment I_{xx}	0.0894	$kg.m^2$
Inertia moment I_{yy}	0.1444	$kg.m^2$
Inertia moment I_{zz}	0.1620	$kg.m^2$
Inertia moment I_{xz}	0.014	$kg.m^2$

A summary of the UAV platform physical properties is given in Table 1. The initial conditions of the state variables are :

$$h(0)=100m, \theta(0)=\phi(0)=\psi(0)=0deg, V(0)=17\,m/s$$
$$p(0)=q(0)=r(0)=0deg/s$$

In addition, the initial values applied in adaptive laws are, $\hat{\sigma}(0)=0.7^*\sigma$, $\hat{\tau}(0)=0.7^*\tau$. In order to demonstrate the performance of the ASMC algorithm, another configuration based on the PID controllers, for both the inner and outer loops, is used in the nonlinear simulation model. Note that the PIDs gains are tuned by trial and error. As a means to clearly demonstrate the actual responses of the system variables and the tracking trajectory, we first simulate the situation without the disturbances. It is illustrated clearly in Figs. 3 and 4 that the designed adaption laws using Lyapunov method had been able to estimate unknown parameters, according to initial values of parameters and gain of adaptation laws, which are defined by the operator.

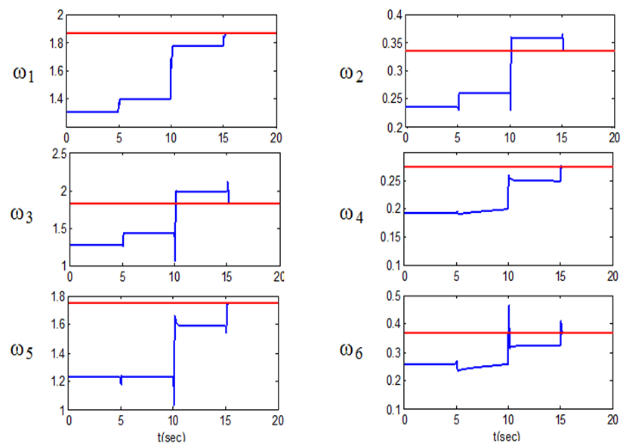

Fig. 3 Parameters estimation of the lateral plane (red line: real, blue line: estimated)

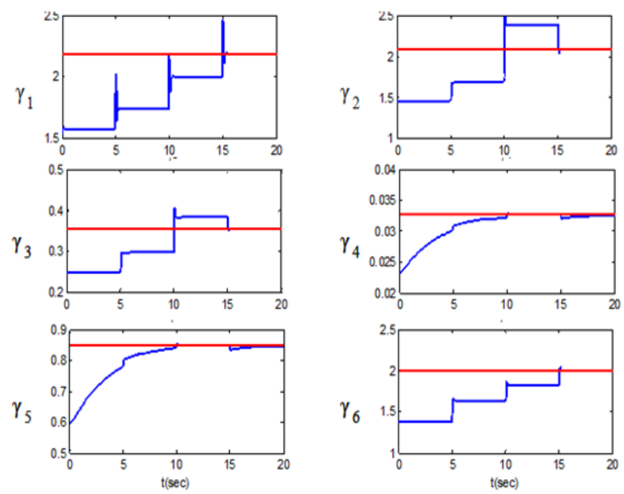

Fig. 4 Parameters estimation of the longitudinal plane (red line: real, blue line: estimated)

Results of the ASMC and the PID algorithm for the inner loops control of small fixed wing UAV are depicted in Fig. 5. The ASMC controller outputs show an excellent tracking of the reference signals for the pitch and roll angles in comparison with the PID controller. Coupling effect of longitudinal and lateral plans results in an overshoot in the PID controller, while the proposed method in this article is free of these drawbacks. In addition, Fig. 6 shows that elevator and aileron deflections of both algorithms remain under the imposed command saturation limit of 20 degrees.

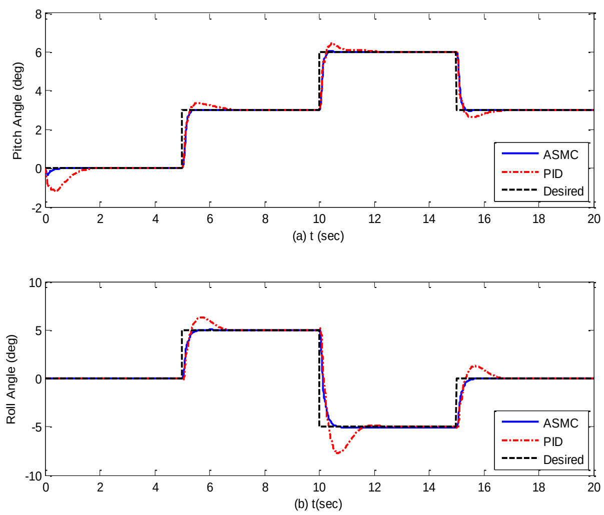

Fig. 5 Inner loops variables, PID and ASMC Confrontation

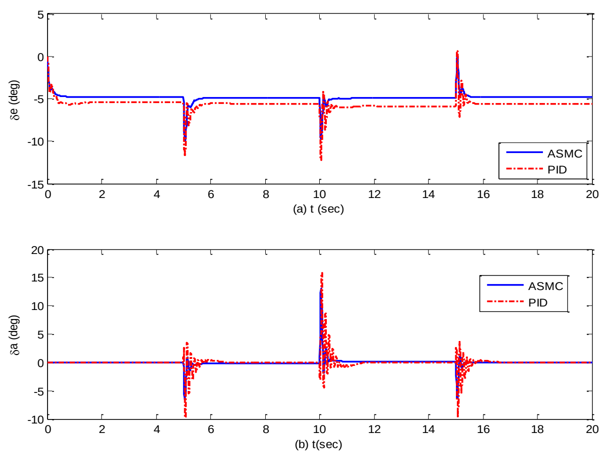

Fig. 6 Inner loops control surfaces, PID and ASMC confrontation

The comparison of the results of the inner loops system with the ASMC and the PID algorithms in the presence of 30% and 20% uncertainties in the aerodynamic coefficients and the Inertia moment, respectively, are illustrated in Fig 7. In addition, the disturbances are represented by wind external currents in x, y directions with a magnitude of 5 m/s at t =8s. The control inputs are shown in Fig 8.

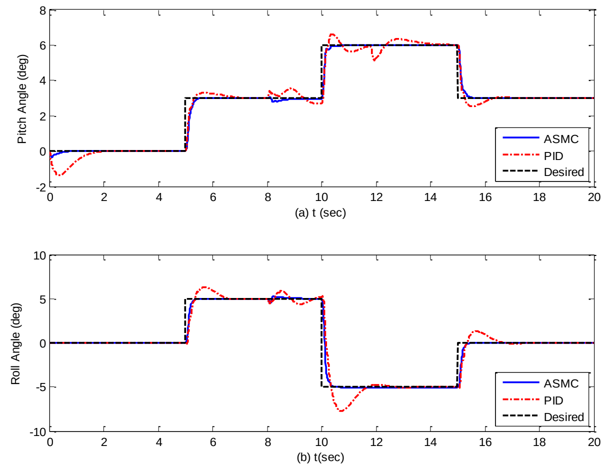

Fig. 7 Inner loops variables under uncertainties and disturbance, PID and ASMC algorithm confrontation

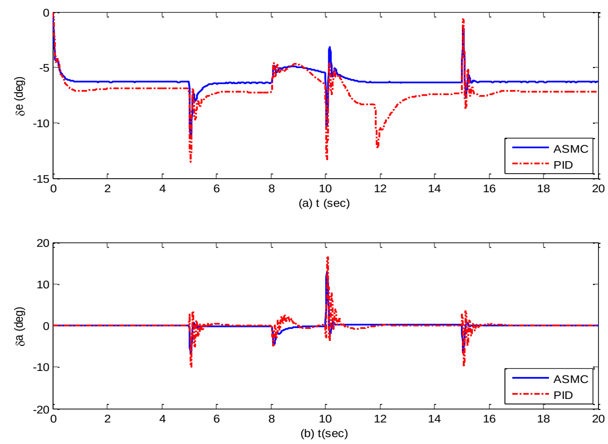

Fig. 8 Inner loops control surfaces under uncertainties and disturbance, PID and ASMC algorithms confrontation

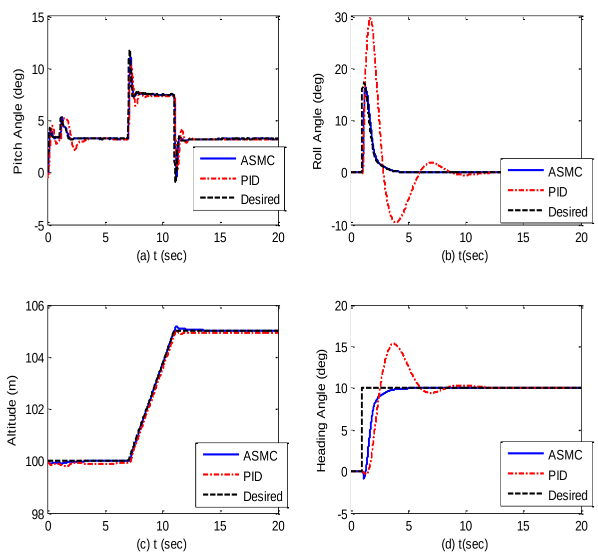

Fig. 9 Nonlinear model variables, PID and ASMC algorithms confrontation

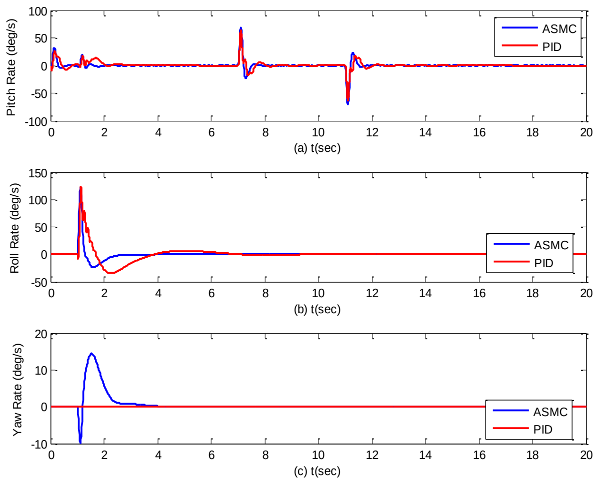

Fig. 10 Nonlinear model angular rates, PID and ASMC algorithms confrontation

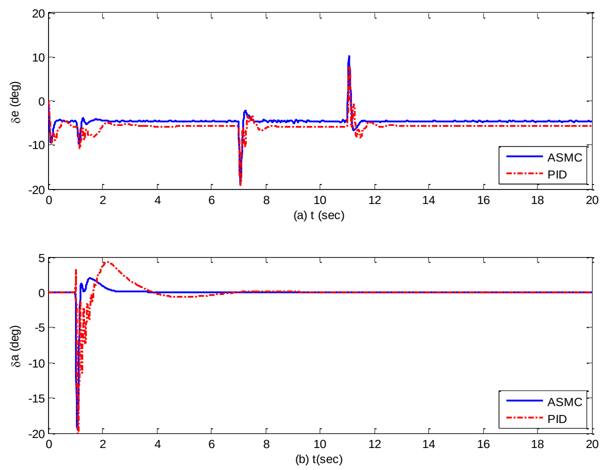

Fig. 11 Nonlinear model control surfaces, PID and ASMC algorithms confrontation

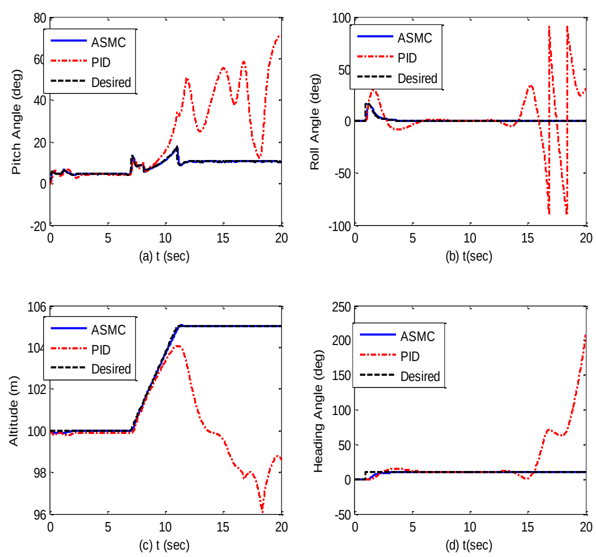

Fig. 12 Nonlinear model variables under uncertainties and disturbance, PID and ASMC algorithms confrontation

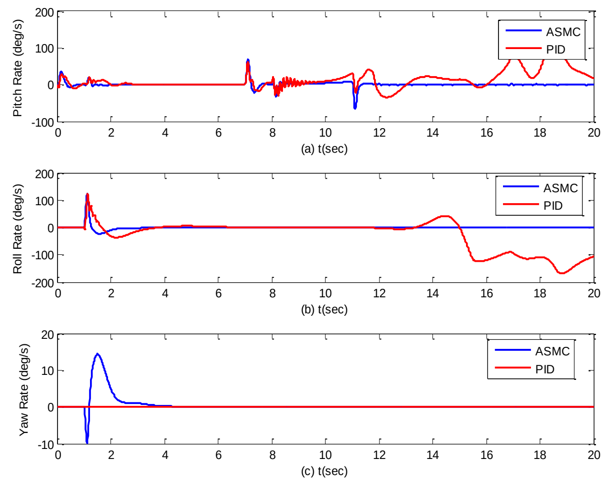

Fig. 13 Nonlinear model angular rates under uncertainties and disturbance, PID and ASMC algorithms confrontation

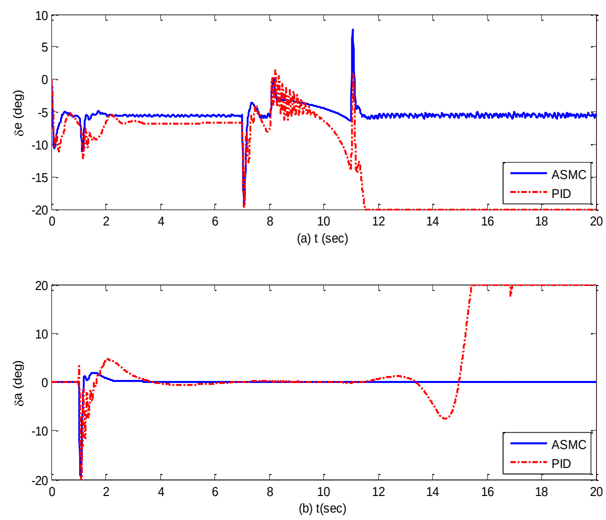

Fig. 14 Nonlinear model control surfaces under uncertainties and disturbance, PID and ASMC algorithms confrontation

It can be concluded that the ASMC controller provides a more robust closed loop system against the uncertainties and disturbances. Fig. 9 illustrates the full nonlinear dynamic responses of the UAV for the applied hybrid ASMC algorithm in comparison with the PID controller. According to this figure, both controllers are able to track the desired trajectories. As far as the stability of the angular rates, the elevator and aileron control surfaces for both controllers in Figs. 10 and 11 confirm this fact. However, the PID controller shows a poor performance on reference changes due to the coupling effect of longitudinal and lateral plans, while the ASMC hybrid model acts better with a more robust inner loop. To verify the proposed method, the UAV is tested in the presence of 20% uncertainties and wind disturbances with a magnitude of 5m/s at t=8s in x direction. As in Fig. 12 can be seen, the adaptive sliding mode control acting on the UAV results an increase in the robustness of the system against uncertainties and disturbances, while the poor performance of the PID linear controller caused the UAV to diverge from its path. The stability of the angular rates, the elevator and aileron control surfaces, presented in Fig. 13 and 14 for the ASMC method, compared to the PID method, confirm the obtained results.

5 CONCLUSION

In this paper, an adaptive sliding mode algorithm employed as the inner loops controller for longitudinal and lateral plans of small fixed wing UAV is analyzed. Firstly, the mathematical model of UAV's attitude motion is derived from the Newton-Euler formulation, including the kinematics and dynamics equations. The modelling of UAV is then implemented in Matlab Simulink environment. In order to achieve the control objective, sliding mode control laws are designed and the unknown parameters of the corresponding controller are estimated through adaptive laws. The global asymptotical stability of the closed-loop system is proved by a Lyapunov based stability analysis. The ASMC algorithm is designed on the inner loops of the UAV dynamics which separates the longitudinal and lateral planes. The ASMC method is chosen for controlling the inner navigation loops. The control variables include the pitch angle θ and roll angle ϕ. Altitude h and heading ψ outer navigation loops are instead controlled by simple PIDs. The simulation results indicate that the attitude and altitude ASMC algorithm can achieve excellent tracking of the reference signals and strong robustness with respect to parametric uncertainties and external disturbance.

6 ACKNOWLEDGMENTS

The authors would like to thank Dr. Masoud Goharimanesh for his comments and suggestions to improve the clarity of this article.

REFERENCES

[1] Clough, B. T., "Unmanned Aerial Vehicles: Autonomous Control Challenges, a Researcher's Perspective", Journal of Aerospace Computing, Information, and Communication 2, Vol. 8, 2005, pp. 327-347.

[2] Giulietti, F., Pollini, L., and Innocenti, M., "Autonomous Formation Flight", IEEE Control Systems Magazine, Vol. 20, 2000, pp. 34-44.

[3] Ryan, A., Zennaro, M., Howell, A., Sengupta, R., and Hedrick, J. K., "An Overview of Emerging Results in Cooperative Uav Control", In: Proceeding of IEEE Conference Decision and Control, 2004, pp. 602-607.

[4] Tadeo, E., Dzul, A., and Llama, M., "Linear And Nonlinear Controllers Applied To Fixed-Wing Uav", International Journal of Advanced Robotic Systems, Vol. 10, No. 33, 2013.

[5] Capello E., Guglieri G., Quagliotti F., and Sartori D., "Design and Validation of an L1 Adaptive Controller for Mini- UAVautopilot", Journal of Intelligent and Robotic Systems, Vol. 69, 2013, pp. 109-118.

[6] Wang E., Jianying, K., and Zhaowei Sun, T., "6-DOF Robust Adaptive Terminal Sliding Mode Control for Spacecraft Formation Flying", Acta Astronautica, Vol. 7, No. 3, 2012, pp. 76-87.

[7] Bin, X., Guo, J., and Zhang, Y., "Adaptive Backstepping Tracking Control of a 6-DOF Unmanned Helicopter", Automatica Sinica, IEEE/CAA Journal of , Vol 2, No. 1, 2015, pp. 19-24.

[8] Babaei A. R., Mortazavi M., and Moradi M. H., "Classical and Fuzzy-Genetic Autopilot Design for Unmanned Aerial Vehicles", Applied Soft Computing Journal, Vol. 11, No. 1, 2011, pp. 365-372.

[9] Shin, D. H., Kim, Y., "Reconfigurable Flight Control System Design Using Adaptive Neural Networks", IEEE Trans. Control System Technol, Vol. 12, No. 1, 2004, pp. 87-100.

[10] Yang, Y. N., Wu J., and Zheng, W., "Attitude Control for a Station Keeping Airship Using Feedback Linearization and Fuzzy Sliding Mode Control", International Journal of Innovative Computing, Information and Control, Vol. 8, No .12, 2012, pp. 8299-8310.

[11] Alessandro, P., Elio, U., "Sliding Mode Control: A Survey With Applications In Math", Journal of Mathematics and Computers in Simulation, No. 81, 2011, pp. 954-979.

[12] Hong, T. K., Youkyung, H. L, and Youdan, K., "Integrated Design of Rotary UAV Guidance and Control Systems Utilizing Sliding Mode Control Technique", International Journal of Aeronautical and Space Sciences, Vol. 13, No. 1, 2012, pp. 90-98.

[13] Modirrousta A., Sohrab M. and Seyed Dehghan M., "Free Chattering Sliding Mode Control With Adaptive Algorithm for Ground Moving Target Tracking", Robotics and Mechatronics (ICRoM), Second RSI/ISM International Conference on. IEEE, 2014.

[14] Bouadi, Hakim, et al, "Adaptive Sliding Mode Control for Quadrotor Attitude Stabilization and Altitude Tracking", Computational Intelligence and Informatics (CINTI), IEEE 12th International Symposium on. IEEE, 2011.

[15] Bouadi, Hakim, et al, "Flight Path Tracking Based-on Direct Adaptive Sliding Mode Control", Intelligent Vehicles Symposium (IV), IEEE, 2011.

[16] Modirrousta, A. Khodabandeh, M., "A Novel Nonlinear Hybrid Controller Design for an Uncertain Quadrotor with Disturbances", Aerospace Science and Technology, Vol. 45, 2015, pp. 294-308.

[17] Daewon, L., Jin Kim, H. and Sastry, Sh., "Feedback Linearization Vs. Adaptive Sliding Mode Control for a Quadrotor Helicopter", International Journal of Control, Automation and Systems, Vol.7, No.3, 2009, pp. 419-428.

[18] Rajagopal, K., Bin S. N., “Robust Adaptive Control of a General Aviation Aircraft”, AIAA Guidance, Navigation, and Control Conference, Toronto, Ontario Canada, 2-5 August 2010.
[19] Moosavian, A., Papadopoulos, E., “Free-Flying Robots In Space: an Overview of Dynamics Modeling, Planning And Control”, Robotica, Vol. 25, No. 5, 2007, pp. 537–547.
[20] Karakas. D., “Nonlinear Modeling and Flight Control System Design of an Unmanned Aerial Vehicle”, Thesis, Middle Esat Technical University, 2007.
[21] Beard. W. R., McLain. T, “Small Unmanned Aircraft: Theory and Practice”, Princeton University Press, 2012.
[22] Roskam, J., “Airplane Flight Dynamics and Automatic Flights, Pt. 1”, DARcorporation, 1995.
[23] Paw, Y. C., Gary, J. B., “Development And Application of an Integrated Framework for Small UAV Flight Control Development”, Journal of Mechatronics, Vol. 21, No. 5, 2011, pp. 789-802.
[24] Paw Y. C., “Synthesis and Validation of Flight Control for UAV”, Dissertation submitted to the Faculty of the Graduate School of the University of Minnesota, December 2009.
[25] Kim, Jin H., David H. S., “A Flight Control System for Aerial Robots: Algorithms And Experiments”, Control Engineering Practice, Vol. 11, No. 12, 2003, pp. 1389-1400.
[26] Utkin, K., Vadim, I., “Sliding Mode Control”, Variable Structure Systems, from Principles To Implementation 66, 2004.
[27] Bartolini, Giorgio, et al, “A Survey of Applications of Second-Order Sliding Mode Control to Mechanical Systems”, International Journal of control, Vol. 76, No. 9-10, 2003, pp. 875-892.